Anomalous electromagnetic response in the spin-triplet superconductor UTe_2

Yusei Shimizu,[1,*] Shunichiro Kittaka,[2] Yohei Kono,[2] Toshiro Sakakibara,[3] Kazushige Machida,[4] Ai Nakamura,[1] Dexin Li,[1] Yoshiya Homma,[1] Yoshiki J. Sato,[1] Atsushi Miyake,[3] Minoru Yamashita,[3] and Dai Aoki[1]

[1]*Institute for Materials Research (IMR), Tohoku University, Oarai, Ibaraki 311-1313, Japan*
[2]*Department of Physics, Chuo University, Kasuga, Bunkyo-ku, Tokyo 112-8551, Japan*
[3]*Institute for Solid State Physics (ISSP), University of Tokyo, Kashiwa, Chiba 277-8581, Japan*
[4]*Department of Physics, Ritsumeikan University, Kusatsu, Shiga 525-8577, Japan*

(Received 15 August 2022; revised 9 December 2022; accepted 12 December 2022; published 23 December 2022)

The recently discovered heavy-fermion superconductor UTe_2, as a promising candidate for an odd-parity superconductivity, exhibits anomalous magnetic-field reinforced superconductivity with a huge upper critical field of 35 T. However, the thermodynamic properties of this unconventional superconductivity still remain unclear. Herein we present the results of dc magnetization and heat capacity measurements in UTe_2 to probe the magnetic response at low temperatures. The obtained isothermal magnetization in the superconducting state of UTe_2 clearly demonstrates the anomalous magnetic flux pinning effect, which is most likely related to the peculiar electromagnetic response of the spin-triplet pairing state in the hard-magnetization axis (orthorhombic *b* axis). The ac susceptibility measurements support the anomalous vortex states in UTe_2. We also found evidence for the Lifshitz transition just above H_{c2} and the anomalous flux pinning anomalies for the easy-magnetization axis (*a* axis).

DOI: 10.1103/PhysRevB.106.214525

I. INTRODUCTION

Unconventional superconductivity with a spin-triplet pairing state has attracted considerable interest because of its unusual nontrivial superconducting (SC) order parameters and magnetic response, which are quite different from those of conventional Bardeen-Cooper-Schrieffer superconductors. In particular, the spin-triplet pairing state protected by a topological invariant provides a good opportunity to seek so-called Majorana fermions, which are believed to appear near the edges of topological superconductors and insulators. In strongly correlated electron systems, the occurrence of a spin-triplet pairing is rare, and it has been extensively examined in uranium heavy-fermion superconductors UBe_{13} and UPt_3 [1–3], and uranium ferromagnetic superconductors, that is, UGe_2, URhGe, and UCoGe [4–8]. Interestingly, the spin-triplet pairing state often appears in correlated $5f$ electron states, although the pairing mechanisms have not been clearly understood from a microscopic point of view.

The recent discovery of unconventional superconductivity in UTe_2 by Ran *et al.* [9] has provided a new opportunity in the research of spin-triplet superconductivity in solid state physics. This material, which crystallizes in the body-centered orthorhombic structure with the space group *Immm* (No. 71, D_{2h}^{25}), exhibits a clear SC transition at $T_{sc} = 1.6$–2 K with a large specific heat jump out of the heavy-fermion paramagnetic state ($C_{ele}/T \sim 0.12\ \mathrm{J\,K^{-2}\,mol^{-1}}$) [9,10]. The magnetic susceptibility shows a remarkable anisotropy without magnetic order down to low temperatures, and the magnetic fluctuations may be related to the significantly anisotropic upper critical field H_{c2} [9–11]. Quite interestingly, the upper critical field for one of the hard-magnetization axes ($H \parallel b$) exhibits an anomalous field-reinforced superconductivity that highly exceeds the Pauli-limiting field, which is followed by the abrupt suppression of the SC state above the first-order metamagnetic transition at 35 T [12–15]. Such a large upper critical field implies the occurrence of the spin-triplet pairing state in UTe_2, which is also supported by recent NMR Knight-shift measurements [16–18]. Furthermore, it has been revealed from the heat capacity [19], magnetic penetration depth [20,21], thermal conductivity [22], and scanning tunneling microscopy (STM) [23] measurements that the SC gap function possesses point nodes along the easy-magnetization direction (*a* axis). Such a point nodal gap structure along with the pressure-induced multiple SC phases [24–26] suggests that the SC order parameter is of nontrivial type, supporting a spin-triplet superconductivity scenario.

One of the most important questions for UTe_2 is an understanding of its thermodynamic behavior and its magnetic response in spin-triplet pairing. A reentrant superconductivity or field-reinforced SC state (upward curvature of the upper critical field) has also been reported in uranium ferromagnetic superconductors URhGe, UCoGe, and UGe_2 [4–8]. It is believed that the interplay of Ising-type ferromagnetic fluctuations and Fermi-surface reconstruction plays a crucial role in driving reentrant superconductivity in these uranium ferromagnetic superconductors. However, the thermodynamic behavior of the reentrant SC state remains elusive because the diamagnetic response of superconductivity is very weak owing to the presence of long-range ferromagnetic ordering. In

*yusei.shimizu.a5@tohoku.ac.jp

UTe_2, the high magnetic field boosted superconductivity occurs from the paramagnetic state, which is a good opportunity to reveal the diamagnetic signals of spin-triplet superconductivity.

In this paper, to gain insight into the spin-triplet superconductivity in UTe_2 from a thermodynamic point of view, we examined static dc magnetization at low temperatures down to 80 mK, using a capacitively detected Faraday magnetometer for $H \parallel a$ and $H \parallel b$. Moreover, we present the results of low-temperature heat capacity measurements in fields up to 13 T, using a specially designed heat capacity cell.

II. EXPERIMENTAL PROCEDURES

Single-crystalline samples of UTe_2 (No. 1 and No. 2, of weights 3.9 and 5.9 mg, respectively) were grown using the chemical vapor transport method, and the crystal axes were characterized using Laue x-ray photographs. Low-temperature magnetization measurements were performed down to 80 mK using a capacitively detected Faraday magnetometer [27,28] installed in ^{3}He-^{4}He dilution and ^{3}He refrigerators, using newly developed high-sensitivity capacitive transducers [28]. Uniform magnetic fields were applied along the orthorhombic a and b axes, and $M(H, T)$ scans were measured with a magnetic-field gradient of $G = 5$ T/m [27,28]. In this study, the influence of the demagnetization is negligible because the magnetic field was applied parallel to the flat c-plane surface of the samples with a thin-plate geometry for both $H \parallel a$ and $H \parallel b$. Low-T heat capacity measurements were performed using a standard quasiadiabatic heat-pulse method at temperatures down to 80 mK in the ^{3}He-^{4}He dilution refrigerator under fields up to 14.5 T for the hard-magnetization axis $H \parallel b$. The platform of the heat capacity cell was fixed by carbon rods to prevent the UTe_2 sample from tilting in magnetic fields for $H \parallel b$ by the strong magnetic anisotropy of UTe_2 [29].

As a complementary approach, we also performed ac susceptibility measurements for single-crystalline UTe_2 with a similar sample quality, using a top-loading ^{3}He-^{4}He dilution refrigerator at temperatures as low as 30 mK in fields up to 14.7 T. Here, the ac susceptibility was measured with a modulation field of 0.6 mT and a frequency of 52 Hz.

III. RESULTS AND DISCUSSION

In Fig. 1, we present the temperature dependence of the heat capacity of UTe_2 measured at zero and magnetic fields along $H \parallel b$. At zero field, a clear heat capacity jump is observed at $T_{sc} \sim 1.6$ K. The nuclear specific heat contribution of $C_{nuc}/T = 0.135H^2/T^3$, coming from ^{123}Te (natural abundance 0.9%) and ^{125}Te (7%), is subtracted for the data taken under magnetic fields.

As shown in Fig. 1, the temperature dependence of C/T shows an upturn at low fields and at high magnetic fields, indicating a non-Fermi-liquid increase of C/T of the normal state. We found that this upturn behavior of C/T observed for $H \parallel b$ is more enhanced than that for $H \parallel a$ at very low temperatures [19]. This anisotropic increase of C/T implies the presence of magnetic fluctuations specific for $H \parallel b$. Meanwhile, recent studies [30–32] reveal a decrease of residual C/T in single crystals with a higher $T_{sc} \sim 2$ K, requiring further low-T heat capacity measurements in high fields for $H \parallel b$ in the future.

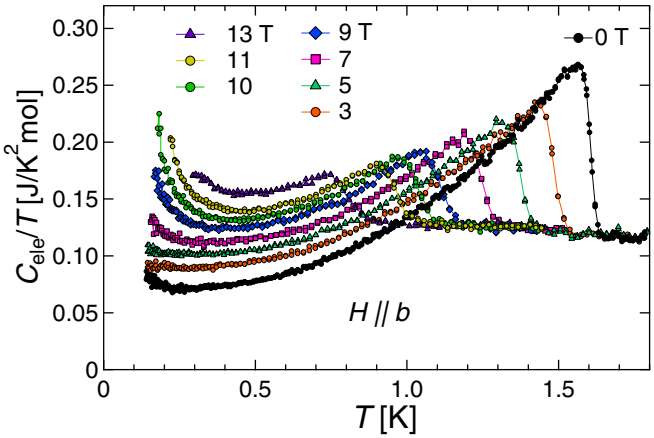

FIG. 1. Temperature dependence of heat capacity in the single-crystalline UTe_2 (No. 1), measured at zero and magnetic fields up to 13 T applied along the orthorhombic b axis. Here, C_{ele}/T denotes the electronic contribution: $C_{ele}/T \equiv [C(T) - C_{nuc}(T)]/T$.

Note that, unlike in recently reported results [33], no significant double transition occurs at T_{sc} in our experimental resolution for the samples used in this study. This absence of a double transition is inconsistent with the SC state with broken time-reversal symmetry suggested by the heat capacity and the Kerr effect measurements [33]. The observed single SC transition in UTe_2 is in contrast to the case of the heavy-fermion superconductor $U_{1-x}Th_xBe_{13}$ [34,35], which is also a promising candidate for spin-triplet superconductivity.

Figures 2(a) and 2(b) show the representative magnetization $[M(H)]$ data of UTe_2 for $H \parallel a$ and $H \parallel b$, respectively. Full field sweeps (increasing and decreasing field sweeps) were performed after zero-field cooling from above T_c. In Fig. 2(a), we show the $M(H)$ curve for $H \parallel a$ along the easy-magnetization axis. Typical diamond-shaped $M(H)$ curves were observed, in agreement with the previous magnetization measurements performed by a superconducting quantum interference device (SQUID) extraction method [36]. The irreversibility of the magnetization curves completely disappears at H_{c2} in UTe_2. In this study, we have found many additional anomalies in $M(H)$. Figures 2(c) and 2(d) show the differential magnetization, $dM(H)/dH$, obtained at several temperatures, for $H \parallel a$ and $H \parallel b$, respectively. For both increasing and decreasing processes of $dM(H)/dH$ at 0.28 K, a sharp cusp anomaly (H_a^*) and a small kink anomaly (H_a^{**}) were observed at $\sim$3 and 0.8 T, respectively. The reason why we observed more anomalies compared to the previous results may be ascribed to the difference in the measuring methods. In the extraction method, the mechanical motions of the sample may cause a tiny field change in the sample, which is unfavorable for measuring systems with irreversible behavior. As observed in the differential magnetization, dM/dH in Fig. 2(c), there is also a broad steplike anomaly at 6 T, just above $\mu_0 H_{c2} = 5.6$ T. This anomaly still exists as a crossover, even at 2 K, well above the SC transition, and does not shift with increasing temperature. The observed anomaly at $\mu_0 H_{Lifshitz} = 6$ T is considered to originate from the Lifshitz

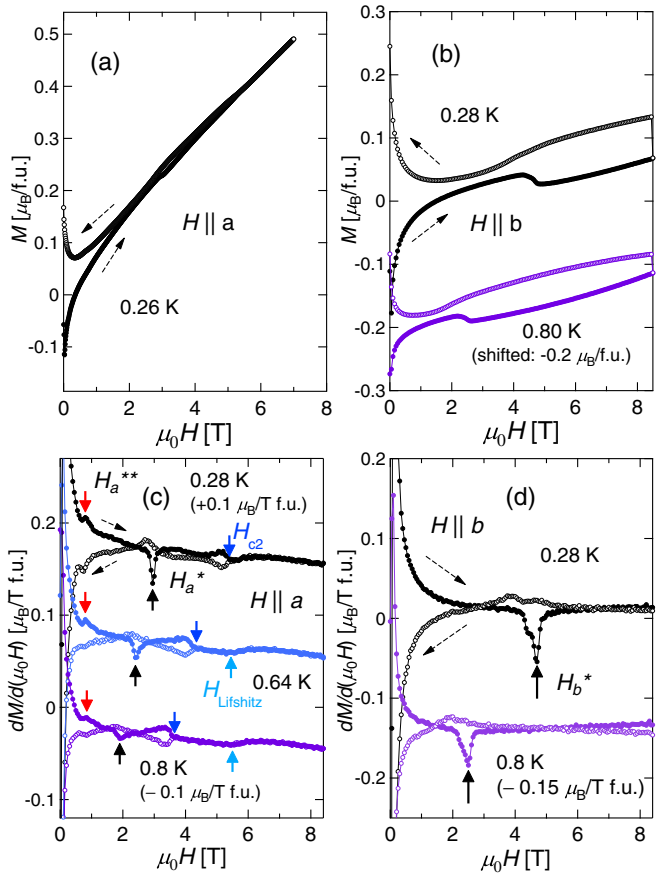

FIG. 2. (a) Magnetization curves $M(H)$ of UTe_2 (No. 2) in fields along $H \parallel a$ at 0.26 K. (b) The $M(H)$ curves of UTe_2, at 0.28 and 0.80 K in fields up to 8.5 T (No. 1) applied along $H \parallel b$, where the data for 0.80 K are shifted vertically for clarity. The shifted values are shown with the data. The differential of magnetization curves, i.e., $dM(H)/dH$, are plotted for increasing and decreasing processes for (c) $H \parallel a$ (0.28, 0.64, and 0.80 K) and (d) $H \parallel b$ (0.28 and 0.80 K). The dashed arrows indicate the increasing and decreasing processes.

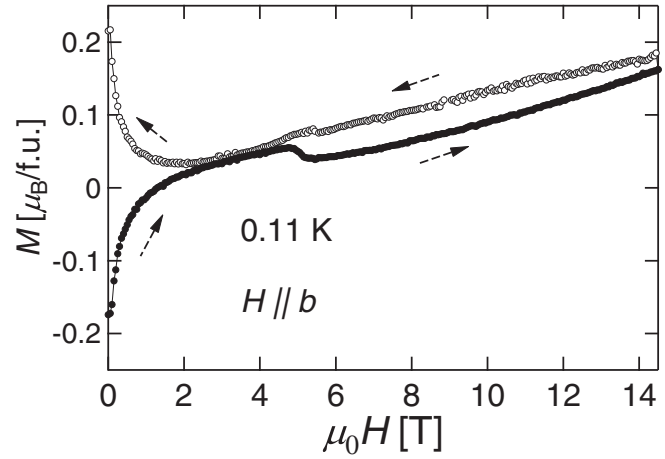

FIG. 3. Magnetization curves $M(H)$ of UTe_2 (No. 1) in fields along $H \parallel b$ at 0.11 K. The dashed arrows indicate the field sweep direction.

transition, and is consistent with previous high-field magnetization [12] and thermoelectric power measurements [37].

Figure 2(b) shows the $M(H)$ data for $H \parallel b$ in the SC state at 0.28 K. Below 1 T, a remarkable hysteresis appears in $M(H)$ between increasing and decreasing sweeps due to the flux pinning effect. This hysteresis rapidly decreases in amplitude and becomes small at approximately 2 T. Interestingly, the $M(H)$ data in the increasing field sweep clearly show a drop at $\mu_0 H_b^* \sim 5$ T. At higher fields, a hysteresis of a nearly constant amplitude appears again and continues up to 14.5 T, the highest field in this experiment. In Fig. 3, we also present $M(H)$ data for $H \parallel b$ in the SC state, measured at a lower temperature of 0.11 K. The noise level of the magnetization data shown in Fig. 3 was slightly higher than that in Fig. 2 owing to the different setup used for the high-field measurements up to 14.5 T. The $M(H)$ curve obtained at 0.11 K shows a clear anomaly at $\mu_0 H_b^* \sim 6$ T. In a decreasing field sweep, the anomaly of $M(H)$ at H_b^* is much smaller than that observed in the increasing field sweep. This behavior of $M(H)$ is at odds with the ordinary peak effect in type-II superconductors, in which the hysteresis appears close to H_{c2} and is symmetrical with respect to the field sweep directions, as in the case of UBe_{13} [38] and UPt_3 [39]. With increasing temperature, H_b^* shifts to lower fields as shown in Fig. 2(d).

The maximum field of the present experiment was 14.5 T (Fig. 3), much lower than H_{c2} for $H \parallel b$. This might have caused an unusual vortex distribution within the sample during the decreasing field sweep. To rule out this possibility, we also measured the decreasing field $M(H)$ data with a different protocol. After measuring the increasing field data, the magnetic field was held at 14.5 T. We then performed a field cooling from above T_c at this field, and subsequently measured the decreasing field $M(H)$ at ~ 0.1 K. The results were exactly the same as those shown in Fig. 2(b) (not shown). The absence of a difference between the field-cooling and the zero-field-cooling measurements shows that the unusual history dependence of $M(H)$ shown in Figs. 2(b) and 2(c) is intrinsic to UTe_2, and that the pinning properties shown by the hysteresis behavior change through H_b^* [Figs. 2(b), 3, and 4]. It would be very important to check this magnetization hysteresis for UTe_2 samples with higher $T_{SC} \sim 2$ K obtained by the NaCl+KCl flux method [31]. While the higher T_{SC} samples with a high residual resistance ratio (RRR) and low residual specific heat can be grown using this method, the obtained UTe_2 samples often include ferromagnetic impurities of U_7Te_{12} ($T_{Curie} = 47$ K) and U_3Te_5 ($T_{Curie} = 120$ K) [31]. In fact, the vortex states in UTe_2 are strongly affected by the above ferromagnetic impurities: An extrinsic hysteresis due to ferromagnetic impurities can occur in the $M(H)$ curve and an inherent hysteresis in the vortex states becomes obscure. A number of experiments and a careful analysis are needed to verify the essential behaviors of magnetization curves in higher-T_{sc} UTe_2 samples, which is left for future study.

Figure 4 shows the temperature dependence of magnetization $M(T)$ in constant fields applied along the hard-magnetization b axis. After zero-field cooling, a warming up to ~1.8 K and a subsequent cooling were performed at each field. At 2 T, the $M(T)$ curve shows a convex upward curvature with the rapid decrease of the SC diamagnetic signal in the warming process. At 3 T, the irreversibility of the magneti-

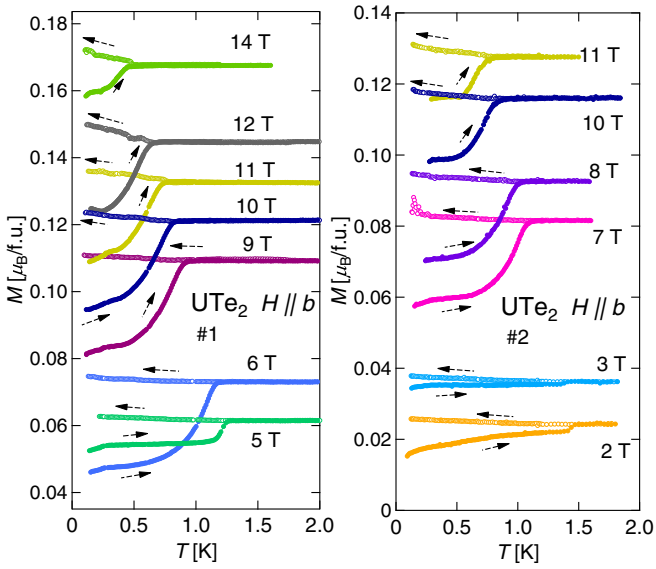

FIG. 4. Temperature dependence of magnetization $M(T)$ of single-crystalline UTe_2, measured at constant fields for No. 1 ($\mu_0 H = 5$, 6, 9, 10, 11, 12, 14 T) and No. 2 ($\mu_0 H = 2$, 3, 7, 8, 10, 11 T), applied along the orthorhombic b axis. The solid and the open symbols show the data obtained in the warming up process after zero-field cooling and that obtained in subsequent cooling process, respectively (dashed arrows).

zation becomes very weak. Above 7 T, a strong irreversibility appears again in $M(T)$ and continues to near $T_c(H)$. These results are consistent with the magnetization data in Fig. 2, indicating that a strong flux pinning occurs above H_b^*.

The strong pinning effect and the anomalous vortex state in UTe_2 are also evidenced by the ac susceptibility (χ_{ac}) data. Figures 5(a) and 5(b) show the magnetic field dependences

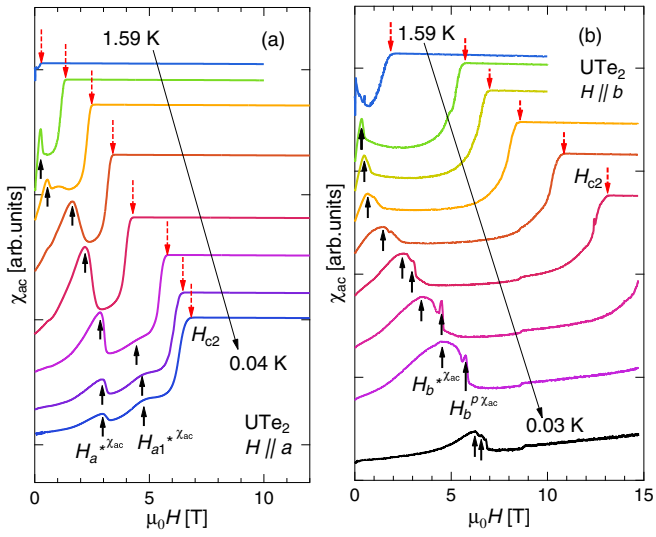

FIG. 5. Magnetic field dependences of ac susceptibility in UTe_2 for (a) $H \parallel a$ ($T = 0.04$, 0.2, 0.4, 0.8, 1, 1.2, 1.39, and 1.59 K) and (b) $H \parallel b$ ($T = 0.03$, 0.4, 0.6, 0.8, 1, 1.2, 1.29, 1.39, and 1.59 K). The solid and dashed arrows indicate the anomalies inside the SC state and the upper critical field, respectively.

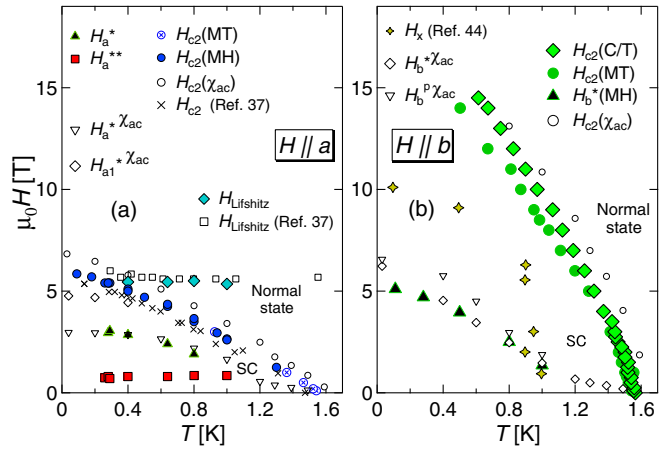

FIG. 6. H-T SC phase diagram of UTe_2 in magnetic fields applied along (a) the easy-magnetization axis $H \parallel a$ and (b) the hard-magnetization axis $H \parallel b$, obtained from the present dc magnetization, ac susceptibility, and heat capacity measurements. The previously published data taken from Refs. [37,44] are also plotted for comparison.

of χ_{ac}, measured at several temperatures down to 0.03 K, for $H \parallel a$ and $H \parallel b$, respectively. For $H \parallel a$, two anomalies were observed at 3 and 4.7 T as indicated by the solid arrows, which are denoted by $H_a^{*\chi_{ac}}$ and $H_{a1}^{*\chi_{ac}}$, respectively. For $H \parallel b$, the ac susceptibility shows an anomaly in higher fields at 6 T for the lowest-temperature data, which is denoted by $H_b^{*\chi_{ac}}$. Moreover, a sharp cusp (peak) also appears at $H_b^{p\chi_{ac}}$ just above $H_b^{*\chi_{ac}}$, which is fully consistent with static dc magnetization results as observed in the dM/dH data at 0.28 K [Fig. 2(d)]. These anomalies shifted to a lower field with increasing temperature [Figs. 5(a) and 5(b)], in agreement with the dc magnetization data.

Figures 6(a) and 6(b) present the obtained SC phase diagram in UTe_2 for $H \parallel a$ and $H \parallel b$, respectively. The SC transition temperatures were determined using the dc magnetization, ac susceptibility, and heat capacity measurements. The initial slope of $H_{c2}(T)$ below 1 T is much larger for $H \parallel b$ than that for $H \parallel a$, indicating a significant difference in the effective mass. In the H-T phase diagram, we have also plotted the H^* for $H \parallel a$ and $H \parallel b$, where the anomalous strong pinning effect occurs in the SC mixed state. The anomalies observed in the ac susceptibility, as denoted by $H_a^{*\chi_{ac}}$ and $H_b^{*\chi_{ac}}$, are in good agreement with the dc magnetization results. The presence of anomalies in the SC state has also been reported for $H \parallel b$ in the NMR studies [16], but the anomalies for $H \parallel a$ have not been reported previously. These anomalies, denoted by H_b^*, have not been detected by heat capacity measurements, suggesting that it is not a phase transition. In addition, we also plotted an additional low-field anomaly (H_a^{**}) at 1 T for $H \parallel a$; currently it is unclear whether this anomaly is due to the flux pinning effect or some type of normal-state anomaly; further studies are necessary to clarify this point. For $H \parallel a$, the observed normal-state anomalies (H_{Lifshitz}) owing to the Fermi-surface reconstruction seem to merge with $H_{c2}(T)$ with decreasing temperature around 6 T. The observed anomaly in the normal state (H_{Lifshitz}) does not show a remarkable temperature dependence, which is in

good agreement with the results of the thermoelectric power measurements [Fig. 6(a)] [37].

Interestingly, the convex upward curvature (bending behavior) of $H_{c2}(T)$ is observed below 4 T for $H \parallel b$, implying the possible presence of the paramagnetic effect in UTe_2 for $H \parallel b$, whereas such a curvature is not observed in $H_{c2}(T)$ for $H \parallel a$. The bending behavior of $H_{c2}(T)$ has also been observed in UBe_{13}, which is a possible candidate for spin-triplet pairing [40]. From the NMR Knight-shift measurements on UTe_2, the spin susceptibility is slightly reduced at T_{sc} for $H \parallel b$ and $H \parallel c$, whereas no significant decrease was observed for the easy-magnetization axis of $H \parallel a$ [18]. In such a triplet-pairing state, the paramagnetic effect may occur when the total spin of the Cooper pair $\boldsymbol{S} \perp \boldsymbol{H}$ is fixed in the crystal direction, which is in good agreement with the convex upward $H_{c2}(T)$ curvature for $H \parallel b$ below 15 T [41].

For $H \parallel b$, the convex upward behavior of $H_{c2}(T)$ becomes less remarkable above 4 T. More specifically, the gradual change of the Knight shift for $6 < \mu_0 H < 12$ T [16] can be understood as the d-vector rotation from a low field ($\boldsymbol{d} \parallel \boldsymbol{H}$) to a high field ($\boldsymbol{d} \perp \boldsymbol{H}$) to gain the Zeeman energy and to avoid the Pauli limit $\mu_0 H_P \simeq 3$ T. In fact, H_{c2} for the b axis exceeds H_P to a large extent. Moreover, a downward $M(H)$ curve expected when H_{c2} is dominated by the Pauli limit [42] is not observed at high fields as shown in Fig. 2(b) and Fig. 3.

In a triplet SC state, the $\boldsymbol{d}$-vector rotation is realized through a topological change in the vortex structure, or the vectorial spin texture consisting of the local Cooper pair spin $\boldsymbol{S}(\boldsymbol{r}) \perp \boldsymbol{d}(\boldsymbol{r})$ in a triplet pairing [43]. As reported by recent NMR studies, the spin contribution of the NMR Knight shift gradually changes from 6 to 12 T [44]. Moreover, the shoulderlike anomalies in the NMR spectra, which indicate the presence of inhomogeneous internal fields, appear above 6 T and disappear at approximately ∼10 T [denoted by H_x in Fig. 6(b)] [44]. These results suggest that the change in the $\boldsymbol{d}$-vector direction does not occur abruptly, and the $\boldsymbol{d}$-vector rotation may occur with anomalous vortex states with inhomogeneous internal fields [44]. The NMR results are fully consistent with our dc magnetization results and the presence of anomalous vortex states in UTe_2. In the higher field $\mu_0 H > 12$ T, the spin moment $\boldsymbol{S}(\boldsymbol{r})$ is fully polarized and uniform along $H \parallel b$ to gain the Zeeman energy; the realized vortex structure would be the same as that in conventional superconductors. In $6 < \mu_0 H < 12$ T, the spin polarization is partial, and the stable state is realized as a spin texture, utilizing the three-dimensional vector degrees of freedom $\boldsymbol{S}(\boldsymbol{r})$. In $0 < \mu_0 H < 6$ T, the $\boldsymbol{d}$ vector is pinned such that $\boldsymbol{d} \parallel \boldsymbol{H}$ and the spin polarization are along the a axis. The strong pinning effect above H_b^* for the $H \parallel b$ axis in Fig. 2(b) might correspond to this depinning field. Further microscopic and theoretical studies are necessary to understand the anomalous vortex state of the spin-triplet pairing in UTe_2. It would be interesting to perform small-angle neutron scattering experiments to probe the internal field distribution at various reciprocal space positions.

IV. SUMMARY

In summary, we performed high-resolution dc magnetization, ac susceptibility, and heat capacity measurements for the easy-magnetization and hard-magnetization axes of UTe_2 to probe the magnetic response of the spin-triplet SC state. The dc magnetization and ac susceptibility data for this unusual SC state clearly demonstrate the anomalous magnetic flux pinning effect, which is most likely related to the peculiarity of the spin-triplet SC state in this material. We found magnetic flux pinning anomalies in the SC mixed state for both $H \parallel a$ and $H \parallel b$ and the Lifshitz transition (Fermi-surface reconstruction) for $H \parallel a$. In addition, we found a remarkable increase in the heat capacity in the low-temperature region in high-magnetic fields when $H \parallel b$, suggesting the possible presence of magnetic fluctuations in UTe_2 reinforced by magnetic fields for $H \parallel b$.

ACKNOWLEDGMENTS

We are grateful to S. Hoshino, Y. Tokunaga, Y. Haga, K. Ishida, and H. Sakai for valuable discussions. The present study was supported by Grants-in-Aid KAKENHI (No. JP20K03851, No. JP21K03455, No. JP17K05553, No. JP20K20889, No. JP20H00130, No. JP22H04933, and No. JP20K03854) from the Ministry of Education, Culture, Sports, Science and Technology (MEXT) of Japan. This work was carried out by the joint research in the Institute for Solid State Physics, the University of Tokyo.

[1] H. R. Ott, H. Rudigier, Z. Fisk, and J. L. Smith, Phys. Rev. Lett. **50**, 1595 (1983).
[2] H. R. Ott, H. Rudigier, T. M. Rice, K. Ueda, Z. Fisk, and J. L. Smith, Phys. Rev. Lett. **52**, 1915 (1984).
[3] G. R. Stewart, Z. Fisk, J. O. Willis, and J. L. Smith, Phys. Rev. Lett. **52**, 679 (1984).
[4] D. Aoki, K. Ishida, and J. Flouquet, J. Phys. Soc. Jpn. **88**, 022001 (2019).
[5] S. S. Saxena, P. Agarwal, K. Ahilan, F. M. Grosche, R. K. W. Haselwimmer, M. J. Steiner, E. Pugh, I. R. Walker, S. R. Julian, P. Monthoux, G. G. Lonzarich, A. Huxley, I. Sheikin, D. Braithwaite, and J. Flouquet, Nature (London) **406**, 587 (2000).
[6] D. Aoki, A. Huxley, E. Ressouche, D. Braithwaite, J. Flouquet, J.-P. Brison, E. Lhotel, and C. Paulsen, Nature (London) **413**, 613 (2001).
[7] F. Levy, I. Sheikin, B. Grenier, and A. D. Huxley, Science **309**, 1343 (2005).
[8] N. T. Huy, A. Gasparini, D. E. de Nijs, Y. Huang, J. C. P. Klaasse, T. Gortenmulder, A. de Visser, A. Hamann, T. Görlach, and H. v. Löhneysen, Phys. Rev. Lett. **99**, 067006 (2007).
[9] S. Ran, C. Eckberg, Q.-P. Ding, Y. Furukawa, T. Metz, S. R. Saha, I.-L. Liu, M. Zic, H. Kim, J. Paglione, and N. P. Butch, Science **365**, 684 (2019).
[10] D. Aoki, A. Nakamura, F. Honda, D. X. Li, Y. Homma, Y. Shimizu, Y. J. Sato, G. Knebel, J.-P. Brison, A. Pourret,

D. Braithwaite, G. Lapertot, Q. Niu, M. Vališka, H. Harima, and J. Flouquet, J. Phys. Soc. Jpn. **88**, 043702 (2019).

[11] S. Ikeda, H. Sakai, D. Aoki, Y. Homma, E. Yamamoto, A. Nakamura, Y. Shiokawa, Y. Haga, and Y. Onuki, J. Phys. Soc. Jpn. **75**, 116 (2006).

[12] A. Miyake, Y. Shimizu, Y. J. Sato, D. X. Li, A. Nakamura, Y. Homma, F. Honda, J. Flouquet, M. Tokunaga, and D. Aoki, J. Phys. Soc. Jpn. **88**, 063706 (2019).

[13] W. Knafo, M. Vališka, D. Braithwaite, G. Lapertot, G. Knebel, A. Pourret, J.-P. Brison, J. Flouquet, and D. Aoki, J. Phys. Soc. Jpn. **88**, 063705 (2019).

[14] G. Knebel, W. Knafo, A. Pourret, Q. Niu, M. Vališka, D. Braithwaite, G. Lapertot, M. Nardone, A. Zitouni, S. Mishra, I. Sheikin, G. Seyfarth, J.-P. Brison, D. Aoki, and J. Flouquet, J. Phys. Soc. Jpn. **88**, 063707 (2019).

[15] S. Ran, I-L. Liu, Y. S. Eo, D. J. Campbell, P. M. Neves, W. T. Fuhrman, S. R. Saha, C. Eckberg, H. Kim, D. Graf, F. Balakirev, J. Singleton, J. Paglione, and N. P. Butch, Nat. Phys. **15**, 1250 (2019).

[16] G. Nakamine, S. Kitagawa, K. Ishida, Y. Tokunaga, H. Sakai, S. Kambe, A. Nakamura, Y. Shimizu, Y. Homma, D. X. Li, F. Honda, and D. Aoki, J. Phys. Soc. Jpn. **88**, 113703 (2019).

[17] G. Nakamine, K. Kinjo, S. Kitagawa, K. Ishida, Y. Tokunaga, H. Sakai, S. Kambe, A. Nakamura, Y. Shimizu, Y. Homma, D. X. Li, F. Honda, and D. Aoki, Phys. Rev. B **103**, L100503 (2021).

[18] H. Fujibayashi, G. Nakamine, K. Kinjo, S. Kitagawa, K. Ishida, Y. Tokunaga, H. Sakai, S. Kambe, A. Nakamura, Y. Shimizu, Y. Homma, D. X. Li, F. Honda, and D. Aoki, J. Phys. Soc. Jpn. **91**, 043705 (2022).

[19] S. Kittaka, Y. Shimizu, T. Sakakibara, A. Nakamura, D. X. Li, Y. Homma, F. Honda, D. Aoki, and K. Machida, Phys. Rev. Res. **2**, 032014 (2020).

[20] S. Bae, H. Kim, Y. S. Eo, S. Ran, I.-l. Liu, W. T. Fuhrman, J. Paglione, N. P. Butch, and S. M. Anlage, Nat. Commun. **12**, 2644 (2021).

[21] K. Ishihara, M. Roppongi, M. Kobayashi, Y. Mizukami, H. Sakai, Y. Haga, K. Hashimoto, and T. Shibauchi, arXiv:2105.13721.

[22] T. Metz, S. Bae, S. Ran, I. L. Liu, Y. S. Eo, W. T. Fuhrman, D. F. Agterberg, S. M. Anlage, N. P. Butch, and J. Paglione, Phys. Rev. B **100**, 220504 (2019).

[23] L. Jiao, S. Howard, S. Ran, Z. Wang, J. O. Rodriguez, M. Sigrist, Z. Wang, N. P. Butch, and V. Madhavan, Nature (London) **579**, 523 (2020).

[24] D. Braithwaite, M. E. Valiska, G. Knebel, G. Lapertot, J.-P. Brison, A. Pourret, M. E. Zhitomirsky, J. Flouquet, F. Honda, and D. Aoki, Commun. Phys. **2**, 147 (2019).

[25] S. M. Thomas, F. B. Santos, M. H. Christensen, T. Asaba, F. Ronning, J. D. Thompson, E. D. Bauer, R. M. Fernandes, G. Fabbris, and P. F. S. Rosa, Sci. Adv. **6**, eabc8709 (2020).

[26] D. Aoki, F. Honda, G. Knebel, D. Braithwaite, A. Nakamura, D. Li, Y. Homma, Y. Shimizu, Y. J. Sato, J.-P. Brison, and J. Flouquet, J. Phys. Soc. Jpn. **89**, 053705 (2020).

[27] T. Sakakibara, H. Mitamura, T. Tayama, and H. Amitsuka, Jpn. J. Appl. Phys. **33**, 5067 (1994).

[28] Y. Shimizu, Y. Kono, T. Sugiyama, S. Kittaka, Y. Shimura, A. Miyake, D. Aoki, and T. Sakakibara, Rev. Sci. Instrum. **92**, 123908 (2021).

[29] S. Nakamura, Doctoral thesis, The University of Tokyo, 2015.

[30] P. F. S. Rosa, A. Weiland, S. S. Fender, B. L. Scott, F. Ronning, J. D. Thompson, E. D. Bauer, and S. M. Thomas, Commun. Mater. **3**, 33 (2022).

[31] H. Sakai, P. Opletal, Y. Tokiwa, E. Yamamoto, Y. Tokunaga, S. Kambe, and Y. Haga, Phys. Rev. Mater. **6**, 073401 (2022).

[32] D. Aoki, H. Sakai, P. Opletal, Y. Tokiwa, J. Ishizuka, Y. Yanase, H. Harima, A. Nakamura, D. X. Li, Y. Homma, Y. Shimizu, G. Knebel, J. Flouquet, and Y. Haga, J. Phys. Soc. Jpn. **91**, 083704 (2022).

[33] I. M. Hayes, D. S. Wei, T. Metz, J. Zhang, Y. S. Eo, S. Ran, S. R. Saha, J. Collini, N. P. Butch, D. F. Agterberg, A. Kapitulnik, and J. Paglione, Science **373**, 797 (2021).

[34] H. R. Ott, H. Rudigier, Z. Fisk, and J. L. Smith, Phys. Rev. B **31**, 1651 (1985).

[35] Y. Shimizu, S. Kittaka, S. Nakamura, T. Sakakibara, D. Aoki, Y. Homma, A. Nakamura, and K. Machida, Phys. Rev. B **96**, 100505 (2017).

[36] C. Paulsen, G. Knebel, G. Lapertot, D. Braithwaite, A. Pourret, D. Aoki, F. Hardy, J. Flouquet, and J.-P. Brison, Phys. Rev. B **103**, L180501 (2021).

[37] Q. Niu, G. Knebel, D. Braithwaite, D. Aoki, G. Lapertot, G. Seyfarth, J.-P. Brison, J. Flouquet, and A. Pourret, Phys. Rev. Lett. **124**, 086601 (2020).

[38] Y. Shimizu, Y. Haga, Y. Ikeda, T. Yanagisawa, and H. Amitsuka, Phys. Rev. Lett. **109**, 217001 (2012).

[39] K. Tenya, M. Ikeda, T. Tayama, T. Sakakibara, E. Yamamoto, K. Maezawa, N. Kimura, R. Settai, and Y. Onuki, Phys. Rev. Lett. **77**, 3193 (1996).

[40] Y. Shimizu, Y. Ikeda, T. Wakabayashi, Y. Haga, K. Tenya, H. Hidaka, T. Yanagisawa, and H. Amitsuka, J. Phys. Soc. Jpn. **80**, 093701 (2011).; Y. Shimizu, Y. Haga, T. Yanagisawa, and H. Amitsuka, Phys. Rev. B **93**, 024502 (2016).

[41] The paramagnetic effect is generally present for the antiparallel pairing state. It occurs even in the triplet pairing state when a magnetic field is applied perpendicular to the direction of total spin of Cooper pairs $\boldsymbol{S}$ (parallel to the $\boldsymbol{d}$ vector).

[42] K. Machida and M. Ichioka, Phys. Rev. B **77**, 184515 (2008).

[43] K. Machida, J. Phys. Soc. Jpn. **89**, 033702 (2020); **89**, 065001 (2020); Phys. Rev. B **104**, 014514 (2021).

[44] G. Nakamine, K. Kinjo, S. Kitagawa, K. Ishida, Y. Tokunaga, H. Sakai, S. Kambe, A. Nakamura, Y. Shimizu, Y. Homma, D. X. Li, F. Honda, and D. Aoki, J. Phys. Soc. Jpn. **90**, 064709 (2021).